

**SURFACE MODIFICATION OF CORN  
STARCH-BASED NANOMATERIALS FOR  
THE ENCAPSULATION OF VITAMIN D3  
AND MAGNESIUM, AND AS  
LEAD AND 2,4DICHLOROPHENOL  
ADSORBENTS**

**AMAL MOHAMMAD AHMAD BADRAN**

**UNIVERSITI SAINS MALAYSIA**

**2025**

**SURFACE MODIFICATION OF CORN  
STARCH-BASED NANOMATERIALS  
FOR THE ENCAPSULATION OF  
VITAMIN D3 AND MAGNESIUM, AND  
AS LEAD AND 2,4DICHLOROPHENOL  
ADSORBENTS**

by

**AMAL MOHAMMAD AHMAD BADRAN**

**Thesis submitted in fulfilment of the requirements  
for the degree of  
Doctor of Philosophy**

**August 2025**

## ACKNOWLEDGEMENT

**First and foremost, thanks to God, for granting me the strength, and patience to face all challenges and complete this journey.**

My deep gratitude to those who have supported and guided me throughout my research until this moment came true.

**Dr. Sapina Abdullah**, I was honored to be her student in USM a long academic life full of success and achievements, for your expert advice and insightful feedback. Your constant support and mentorship have greatly enriched my research experience and contributed significantly to my professional growth.

**Dr. Afif Hethnawi**, for teaching me a lot and guiding me along this topic with his profound knowledge and wisdom. Your invaluable guidance and unwavering support have been instrumental in this accomplishment.

**Dr. Nor Shariffa bt. Yussof**, your encouragement, critical insights, and constructive suggestions have been vital in shaping the direction of this thesis.

**Prof. Fazilah Arrifin**, I will never forget your first lesson emphasizing the importance of honesty and commitment.

**My dear parents**, mercy upon your souls, your values have shaped the person I am today.

I am profoundly grateful to my family for their unwavering love and support. To my special husband **Ismaeil**, your patience, understanding, and constant encouragement have been my foundation throughout this journey.

To my beloved daughters, **Manar, Lujain, Habiba, and Salma**, and my son, **Yazeed**, my source of strength and joy. To my sisters, **Reem, Jihad, Jehan, Abeer, Hiba**, and my brothers, **Ahmad, and Saif**, who believe in me and never stop their love.

**To Raghad & Ahmad for their endless support, and the beloved ones Tareq & Mimi.**

**To ..... Gaza and all martyrs**

**To .... Palestine**, the land of sacrifice & resilience.

## TABLE OF CONTENTS

<b>ACKNOWLEDGEMENT .....</b>	<b>ii</b>
<b>TABLE OF CONTENTS.....</b>	<b>iii</b>
<b>LIST OF TABLES .....</b>	<b>viii</b>
<b>LIST OF FIGURES .....</b>	<b>x</b>
<b>LIST OF SYMBOLS.....</b>	<b>xiii</b>
<b>LIST OF ABBREVIATIONS .....</b>	<b>xiv</b>
<b>LIST OF APPENDICES.....</b>	<b>xvi</b>
<b>ABSTRAK.....</b>	<b>xvii</b>
<b>ABSTRACT .....</b>	<b>xx</b>
<b>CHAPTER 1 INTRODUCTION .....</b>	<b>1</b>
1.1 Background.....	1
1.2 Rationale of the Study .....	3
1.2.1 Problem Statement.....	4
1.2.2 Aim & Objectives.....	5
1.2.3 Hypothesis.....	6
1.3 Thesis Organization (Framework).....	7
<b>CHAPTER 2 LITERATURE REVIEW.....</b>	<b>8</b>
2.1 Introduction.....	8
2.2 Starch.....	11
2.2.1 Starch Identification and Composition .....	11
2.2.1(a) Native and High Amylose Corn Starch.....	13
2.2.2 Physicochemical Properties: Viscosity, Thermal Stability, Crystallization, Retrogradation.....	15
2.2.3 Morphological Characteristics.....	17
2.2.4 Potential Use .....	19

2.2.4(a)	Encapsulation.....	20
2.3	SNPs Structure and Synthesis protocol .....	23
2.3.1	Bottom-Up Protocols .....	25
2.3.2	Top-Down Protocols.....	25
2.3.2(a)	Physical treatment .....	25
2.3.2(a)(i)	Ultrasonication.....	26
2.3.3	Morphology.....	29
2.4	Stability of NP.....	31
2.4.1	Thermodynamic Stability.....	34
2.4.1(a)	Surface Energy (ZP).....	37
2.4.1(b)	Polydispersity Index (PDI) .....	39
2.4.1(c)	Hydrophobicity & Dispersity.....	40
2.4.1(d)	Particle Size .....	42
2.4.1(e)	Morphology and Geometry Affected Stability of SNPs.....	43
2.4.1(f)	Crystallinity .....	45
2.4.2	Enhancing Stability and Thermodynamics .....	46
2.4.2(a)	Improving Functionality of Nano-sized Starch Particles .....	46
2.4.2(b)	Improving Stability Surface loading with VD <sub>3</sub> by Modifying Starch Nanoparticles .....	47
2.5	Encapsulation of Vitamin D <sub>3</sub> .....	48
2.6	Mathematical Modeling.....	49
2.7	Release Performance .....	51
2.8	SNM as Adsorbents for Toxic Compounds .....	53
	<b>CHAPTER 3 SURFACE MODIFICATION AND CHARACTERIZATION OF STARCH-BASED NANOMATERIAL.....</b>	<b>57</b>
3.1	Introduction.....	57

3.2	Materials and Methods .....	58
3.2.1	Materials .....	58
3.2.2	Methods .....	59
3.2.2(a)	Synthesis of starch nanomaterial and surface modification.....	59
3.2.3	Characterization of SNM and MSNM .....	62
3.2.3(a)	X-Ray Diffraction (XRD).....	62
3.2.3(b)	Atomic Force Microscopy (AFM) .....	63
3.2.3(c)	Fourier-Transform Infrared Spectroscopy (FTIR).....	64
3.2.3(d)	BET Surface Area and Porosity Analysis .....	64
3.2.3(e)	Zeta Potential .....	65
3.2.3(e)(i)	Statistical Analysis.....	65
3.3	Results & Discussion.....	65
3.3.1	Characterization.....	66
3.3.1(a)	Structural Identity – XRD.....	66
3.3.1(b)	Particle Size and Uniformity- by AFM.....	68
3.3.1(c)	Functionality- by FTIR.....	70
3.3.1(d)	Textural Property and Pore Size Distribution- by BET .....	72
3.3.1(e)	Zeta Potential .....	75
3.4	Conclusion .....	76
<b>CHAPTER 4 STARCH-BASED NANOMATERIAL AS A DUAL CARRIER FOR MAGNESIUM AND VITAMIN D3: ADSORPTION ISOTHERM, MODELING, AND RELEASE PERFORMANCE.....</b>		<b>78</b>
4.1	Introduction.....	78
4.2	Materials & Method .....	80
4.2.1	Materials .....	80
4.2.2	Methods .....	80

4.2.2(a)	Preparation of Phosphate Buffer Solution.....	80
4.2.2(b)	Introducing VD <sub>3</sub> in the Dialysis Bag .....	81
4.2.2(c)	Characterization .....	82
4.2.2(c)(i)	FTIR.....	82
4.2.2(c)(ii)	Zeta Potential.....	82
4.2.2(d)	Adsorption Isotherm and Modeling .....	83
4.2.2(e)	Cumulative Release of VD <sub>3</sub> with the Modified Nanomaterial.....	85
4.3	Results & Discussion.....	88
4.3.1	Characterization.....	88
4.3.1(a)	Functionality – FTIR.....	88
4.3.1(b)	Stability- Zeta-Potential.....	90
4.3.2	Adsorption Isotherm and Modeling.....	92
4.3.3	Release Performance.....	97
4.4	Conclusion .....	100
<b>CHAPTER 5 STARCH-BASED NANOMATERIAL AS ADSORBENT FOR DETOXIFICATION OF LEAD (Pb) &amp; 2,4DICHLOROPHENOLE; ADSORPTION ISOTHERMS, &amp; MODELLING .....</b>		
<b>101</b>		
5.1	Introduction.....	101
5.2	Materials & Method .....	104
5.2.1	Material.....	104
5.2.2	Method.....	104
5.2.2(a)	Synthesis and Modification of Starch-Based Nano Detoxicant.....	104
5.2.2(b)	Characterization of the Adsorbent .....	105
5.2.2(b)(i)	Surface Functionality FTIR.....	105
5.2.2(b)(ii)	Zeta Potential.....	105
5.2.2(c)	Adsorption Isotherm and Modeling .....	106

5.2.2(d)	Adsorption Kinetics .....	109
5.2.2(e)	Regeneration Experiment .....	110
5.3	Results & Discussion.....	110
5.3.1	Characterization.....	110
5.3.1(a)	FTIR .....	110
5.3.2	Adsorption Isotherm.....	115
5.3.3	Adsorption Kinetics.....	120
5.3.4	Regeneration.....	125
5.3.4(a)	Desorption Efficiency.....	125
5.3.4(b)	Re-Adsorption Capacity .....	129
5.4	Conclusion .....	132
<b>CHAPTER 6 CONCLUSION &amp; RECOMMENDATIONS.....</b>		<b>134</b>
6.1	Conclusion .....	134
6.2	Recommendation.....	135
<b>REFERENCES.....</b>		<b>136</b>
<b>APPENDICES</b>		
<b>LIST OF PUBLICATIONS</b>		

## LIST OF TABLES

		<b>Page</b>
Table 2.1	Comparison between amylose and amylopectin in starch.....	12
Table 2.2	Comparison between native and modified starch.....	16
Table 2.3	Scanning electron microscopy, for different types of starch .....	17
Table 2.4	SNP's preparation methodology; top-down and bottom-up.....	24
Table 2.5	Common devices used to measure starch nanoparticle stability.....	32
Table 2.6	Thermodynamic stability for previously investigated nanomaterials.....	35
Table 2.7	Multiple encapsulation techniques for VD <sub>3</sub> and release performance, EE, EL, stability and type of raw material. ....	52
Table 3.1	Zeta potential for the starch nanomaterial (SNM) and after modification (MSNM-Mg) .....	76
Table 4.1	Adsorption isotherm models and their corresponding parameters (Kargi and Pamukoglu, 2003; Li et al., 2019; Malik, 2004).....	84
Table 4.2	Zeta potential (n = 3; error bars: standard deviation) for experimental results for the SNM, MSNM-PM-VD <sub>3</sub> , MSNM-Mg, and MSNM-Mg-VD <sub>3</sub> . PM: physical mixing. The asterisk shows p < 0.05 by t-test .....	91
Table 4.3	Fitting parameters generated by fitting VD <sub>3</sub> with nonlinear fitting of the experimental data using Langmuir and BET isotherm models .....	94
Table 4.4	Summarizes the expected parameters of the effective diffusion coefficient (D <sub>eff</sub> ) and chi-square analysis $\chi^2$ for accumulative release at 37°C and pH 7.4.....	99
Table 5.1	The results of One Way ANOVA of the differences between Zeta potential Measurements (SNM, MSNM-Mg, SNM-2,4DCPh, MSNM-Mg-2,4DCPh).....	114
Table 5.2	Chi-square value, adsorption capacity, and adsorption parameters for SNM-Pb adsorption by Langmuir model .....	117
Table 5.3	Chi-square value and Adsorption parameters for MNM-Mg-Pb adsorption by Freundlich model.....	118

Table 5.4	Fitting parameters generated by fitting SNM-2,4DCPh with nonlinear fitting of the experimental data using Langmuir isotherm model.....	120
Table 5.5	Fitting parameters generated by fitting MSNM-2,4DCPh with nonlinear fitting of the experimental data using BET isotherm models.....	120
Table 5.6	Results of One-way ANOVA of The Differences in Desorption Deficiency Between pH 3, and pH 2.....	126
Table 5.7	The results of independent sample T-test of the differences of desorption efficiency of 2,4 DCPh between pH 9 and pH 10.....	128
Table 5.8	The Results of Independent Sample T-test of The Differences of Adsorption Capacity (mg/g).....	130
Table 5.9	Results of Independent sample T-test of the differences of adsorption capacity between pH 9 and pH 10. ....	131

## LIST OF FIGURES

		<b>Page</b>
Figure 1.1	Research framework .....	7
Figure 2.1	(a) Structural units of starch amylose, and (b). Amylopectin: red is oxygen atom, white is hydrogen atoms, and grey is carbon. ....	12
Figure 2.2	Resistant starch-encapsulated probiotics .....	21
Figure 2.3	The figure shows encapsulation of hydrophobic or low bioactive material in an aqueous phase.....	22
Figure 2.4	SNP's preparation approaches .....	24
Figure 2.5	Scanning electron microscopy (SEM) images of potato starch nanoparticles that have a spherical oval shape .....	30
Figure 2.6	Scanning electron microscopy (SEM) image of corn starch nanoparticles with angular shapes.....	31
Figure 2.7	Thermodynamic stability and steric stability of nanoparticles.....	34
Figure 2.8	Zeta potential.....	37
Figure 3.1	Synthesis and characterization of SNM.....	60
Figure 3.2	Surface modification and characterization of MSNM-Mg .....	62
Figure 3.3	(a). Shows the intensity and $2\theta$ for three samples: bulk starch, nanomaterial (SNM), and modified nanomaterial (MSNM-Mg); (b). XRD- MSNM Match with starch and Mg with code 1 and 80.1 % match; and (c) XRD- MSNM Match with starch alone code 2 with 100 % match. ....	66
Figure 3.4	(a). AFM images of the nanomaterial (SNM), before modification, and (b). AFM images of the nanomaterial after modification with Mg (MSNM-Mg) .....	69
Figure 3.5	(a). FT-IR spectra of the nanomaterial before modification (SNM), nanomaterial after modification with magnesium citrate (MSNM-Mg), and MgO at wavenumber (500–1700) $\text{cm}^{-1}$ ; and (b). FT-IR spectra for the nanomaterial before modification (SNM), nanomaterial after modification with magnesium citrate (MSNM-Mg), and MgO at wavenumber (2800–4000) $\text{cm}^{-1}$ .....	71

Figure 3.6	(a) Adsorption-desorption isotherm and pore size distribution for SNM before preliminary modification with magnesium citrate, and (b). adsorption-desorption isotherm and pore size distribution of the nanomaterial after preliminary modification with magnesium citrate (MSNM-Mg).....	73
Figure 4.1	(a) FT-IR spectra of the nanomaterial before modification (SNM), nanomaterial after modification with magnesium citrate (MSNM-Mg), and MgO at wavenumber (500–1700) $\text{cm}^{-1}$ ; and (b). FT-IR spectra for the nanomaterial before modification (SNM), nanomaterial after modification with magnesium citrate (MSNM-Mg), and MgO at wavenumber (500–1700) $\text{cm}^{-1}$ .....	88
Figure 4.2	(a) Adsorption isotherm for MSNM-Mg fitted the experimental data with the Langmuir model, (b). adsorption isotherm for the modified nanomaterial after final loading with $\text{VD}_3$ (MSNM-Mg- $\text{VD}_3$ ) and the experimental data were fitted with the BET model.....	93
Figure 4.3	Cumulative release of MSNM-Mg- $\text{VD}_3$ , physical mixing of MSNM-Mg with $\text{VD}_3$ , and fitting to a Fickian diffusion model. ....	98
Figure 5.1	(a) FT-IR spectra of the nanomaterial before modification (SNM), SNM-Pb, MSNM-Pb, and Pb acetate at wavenumber (400–1700) $\text{cm}^{-1}$ ; and (b) FT-IR spectra for the nanomaterial before modification (SNM), and SNM-Pb, MSNM-Pb, and Pb acetate at wavenumber (2800-4000) $\text{cm}^{-1}$ .....	111
Figure 5.2	(a). FT-IR spectra for the 2,4DCPh, SNM, MSNM-2,4DCPh, SNM-2,4DCPh at wavenumber (400-1700) $\text{cm}^{-1}$ , (b). FT-IR spectra for the 2,4DCP, SNM, MSNM-Mg, MSNM-2,4DCPh, SNM-2,4DCPh at wavenumber (2800-4000) $\text{cm}^{-1}$ .....	113
Figure 5.3	Adsorption isotherm for the experimental data for lead with SNM presenting Langmuir and Freundlich models .....	116
Figure 5.4	Adsorption isotherm for the experimental data for modified MSNM with Pb presenting Freundlich fitting model.....	117
Figure 5.5	Adsorption isotherm for the experimental data for 2,4DCPh adsorbed on the modified nanomaterial MSNM-Mg presenting BET model.....	120
Figure 5.6	The nonlinear fitting of pseudo-second-order kinetics to our adsorption data for lead (Pb) on the MSNM-Mg. The dots represented the experimental data, while the solid lines came from the fitting model.....	123

Figure 5.7	The nonlinear fitting of pseudo-second-order kinetics to our adsorption data for 2,4DCPh onto MSNM-Mg. The dots expressed experimental data, while the solid lines are from the fitting model.....	125
Figure 5.8	Desorption efficiency of Pb-spent at different pH (3, and 2).....	126
Figure 5.9	FTIR spectra for the spent material (MSNM-Mg-Pb) at wave number from (400-4000) $\text{cm}^{-1}$ at pH 2 and 3.....	127
Figure 5.10	Desorption efficiency of Spent MSNM-2,4DCPh at Different pH (9, 10).....	128
Figure 5.11	Re-adsorption capacity for Pb-spent with different initial concentrations.....	130
Figure 5.12	Re-adsorption capacity for spent MSNM-Mg-2,4DCPh for three cycles at pH 9 & 10.....	131

## LIST OF SYMBOLS

$\text{\AA}$	Angstrom, unit of length, equal to 0.1 nano meter.
$C_e$	Concentration at equilibrium / remaining solute concentration in the solution at equilibrium.
$C_i$	Initial concentrations.
$^{\circ}\text{C}$	Temperature in Celsius
$D_{\text{eff}}$	Diffusivity coefficient
$k_1$	Langmuir constant.
$M$	Molarity.
$M_{\infty}$	the loaded amount of $\text{VD}_3$ on the surface of the nanomaterial
$M_i/M_{\infty}$	the percentage of the cumulative release of all loaded nanomaterial
$Q_{\text{max}}$	Maximum adsorption capacity
$R^2$	Linear regression correlation coefficient.
$V$	Volume.

## LIST OF ABBREVIATIONS

2,4DCPh	2,4Dichlorophenol
AFM	Atomic force microscope
BET	Brunauer–Emmett–Teller.
BPS-E	Buffer Phosphate Solution-Ethanol
C <sub>6</sub> H <sub>8</sub> O <sub>7</sub>	Citric acid
EE	Encapsulation Efficiency
FT-IR	Fourier transforms the infrared spectrum
FWHM	Full width at half maximum is needed to calculate the crystalline domain size.
HACS	High amylose corn starch
K <sub>2</sub> HPO <sub>4</sub>	Potassium dihydrogen phosphate
KH <sub>2</sub> PO <sub>4</sub>	Potassium dihydrogen phosphate
LD <sub>50</sub>	Lethal dose 50%
Mg <sup>2+</sup>	Magnesium
MgO	magnesium oxide
MSNM	Modified starch nanomaterial
MSNM-Mg	Modified starch nanomaterial with magnesium.
MSNM-Mg-2,4DCPh	Modified starch nanomaterial with magnesium and functionalized with 2,4DCPh
MSNM-Mg-Pb	Modified starch nanomaterial with magnesium and functionalized with Pb
MSNM-Mg-VD <sub>3</sub>	Modified starch nanomaterial with magnesium and final functionalized with VD <sub>3</sub>
NCS	Native corn starch
NS	Nano starch
SBNM	Starch-Based Nanomaterial
SNM	Starch Nanomaterial

VD <sub>3</sub>	Vitamin D <sub>3</sub>
WHO	World Health Organization
XRD	X-Ray Diffraction
Z- potential	Zeta potential

## LIST OF APPENDICES

- Appendix A Most reported adsorption isotherm models and their corresponding parameters
- Appendix B Adsorption isotherms for the experimental data of  $\text{VD}_3$  with different fitting models (Toth, Redlich Peterson, Freundlich)

**PENGUBAHSUAIAN PERMUKAAN BAHAN NANO BERASASKAN KANJI  
JAGUNG UNTUK ENKAPSULASI VITAMIN D3 DAN MAGNESIUM  
SERTA SEBAGAI PENJERAP PLUMBUM DAN 2,4-DIKLOROFENOL**

**ABSTRAK**

Para penyelidik telah membangunkan pelbagai strategi untuk menghasilkan suplemen mikronutrien makanan seperti magnesium ( $Mg^{2+}$ ) dan vitamin D<sub>3</sub> (VD<sub>3</sub>), namun berdepan dengan masalah interaksi yang tidak dijangka serta isu keserasian (contohnya, magnesium terhidrat secara perlahan apabila bercampur dengan air, manakala vitamin D<sub>3</sub> bersifat hidrofobik dan memerlukan pembawa dalam larutan berasaskan air). Kanji digunakan secara meluas disebabkan ciri-ciri permukaannya, kebolehaiannya secara biologi, dan keserasiannya. Walau bagaimanapun, kebanyakan kaedah kimia atau fizikal terkini masih belum diuji secara menyeluruh di peringkat makmal, sebahagiannya gagal menghasilkan partikel bersaiz nano yang seragam, tidak cekap, sukar dihasilkan secara berskala besar dan memerlukan pelbagai langkah penghasilan. Kajian ini bertujuan untuk menghasilkan bahan nano kanji jagung (SNM) sebagai pembawa nano yang berkesan untuk VD<sub>3</sub> dan  $Mg^{2+}$ , serta sebagai ejen penyahtoksik nano untuk Pb dan 2,4DCPh. Pada peringkat awal, SNM disediakan melalui proses ultrasonik menggunakan campuran kanji jagung asli dengan kandungan amilosa tinggi dalam nisbah jisim yang sama di bawah keadaan sederhana. SNM yang terhasil kemudian diubah suai dengan magnesium sitrat (MSNM-Mg) sebagai langkah pengubahsuaian utama untuk digunakan sebagai pembawa nano bagi VD<sub>3</sub> dalam kehadiran magnesium. MSNM-Mg dianalisis dari segi saiz, ciri permukaan, fungsi, kestabilan dan morfologi. Seterusnya, kinetik pelepasan bahan ini selepas pemuatan VD<sub>3</sub> terakhir (MSNM-Mg-VD<sub>3</sub>) diuji dalam larutan penimbal

fosfat pada pH 7.4, yang mensimulasikan aliran darah. Akhir sekali, MSNM-Mg diuji sebagai ejen penyahtoksik nano bagi penjerapan Pb dan 2,4DCPh dari tubuh manusia. Tingkah laku penjerapan VD3 dan sebatian toksik (Pb dan 2,4DCPh) pada permukaan MSNM dikaji menggunakan pelbagai model isotherm. Eksperimen penjanaan semula bahan digunakan juga dilakukan dengan variasi pH. Hasil kajian menunjukkan bahawa SNM yang stabil berjaya dihasilkan dengan nilai *Z-potential* sebanyak -36 mV berbanding -30 mV sebelum pengubahsuaian, dengan saiz purata 7 nm. Bahan menjadi kurang berliang selepas pengubahsuaian, dengan pengurangan luas permukaan BET daripada 40 m<sup>2</sup>/g kepada 28 m<sup>2</sup>/g, yang mengesahkan kejayaan penambatan magnesium sitrat pada permukaan. MSNM-Mg-VD3 menunjukkan kestabilan tertinggi dengan *zeta-potential* -41 mV. Pelepasan VD3 sepenuhnya berlaku selepas 5 jam, menunjukkan kebolehsbaran (*Deff*) yang lebih rendah dan pelepasan terkawal yang lebih baik berbanding penjerapan VD3 secara fizikal. Tambahan pula, isotherm penjerapan bagi MSNM menunjukkan tingkah laku penjerapan berlapis (BET), berbanding penjerapan satu lapisan bagi bahan sebelum pengaktifan, yang menyerlahkan kesan pengubahsuaian permukaan dalam meningkatkan penjerapan VD3. MSNM-Mg menunjukkan keupayaan penjerapan Pb dan 2,4DCPh yang sangat baik secara berasingan, masing-masing sebanyak 388 mg/g dan 5600 mg/g, berbanding hanya 121 mg/g dan 300 mg/g bagi SNM, dengan tingkah laku penjerapan berlapis mengikut model Freundlich dan BET. Kinetik penjerapan bagi kedua-dua Pb dan 2,4DCPh hanya memerlukan 10 minit untuk mencapai keseimbangan. Kajian juga menunjukkan kadar pemulihan melebihi 90% bagi kedua-dua bahan penyerap selepas tiga kitaran penjanaan semula. Penemuan ini menyokong andaian bahawa MSNM berpotensi tinggi sebagai penyerap bagi Pb dan 2,4DCPh dengan kadar pemulihan yang tinggi. Hasil yang inovatif ini menyerlahkan kepentingan teknik pengubahsuaian

permukaan dalam meningkatkan kestabilan bahan nano terubah suai serta mengaktifkan tenaga permukaan untuk memaksimumkan keupayaan penjerapan bahan terhadap bahan toksik.

**SURFACE MODIFICATION OF CORN STARCH-BASED  
NANOMATERIALS FOR THE ENCAPSULATION OF VITAMIN D<sub>3</sub> AND  
MAGNESIUM, AND AS LEAD AND 2,4-DICHLOROPHENOL  
ADSORBENTS**

**ABSTRACT**

Researchers have explored ways to deliver micronutrients like magnesium and vitamin D<sub>3</sub>, but issues such as slow hydration and poor water compatibility have limited progress. At the same time, pollutants like lead and 2,4-DCPh pose serious health risks, and conventional removal methods are often costly or unsustainable. Thus, there is a need for safe, eco-friendly, and cost-effective adsorbents to protect public health. This study aims to fabricate starch nanomaterials (SNM) as an effective nanocarrier for VD<sub>3</sub> and Mg<sup>+2</sup>, and as a nano-detoxicant for Pb and 2,4DCPh. Initially, the SNM was prepared by ultrasonication of equal masses of native and high-amylose corn starch under moderate conditions. Consequently, the generated SNM was then grafted with magnesium citrate (MSNM-Mg) as a primary modification step to be used as a nano-carrier for VD<sub>3</sub> in the presence of magnesium. The MSNM-Mg was experimentally analyzed to determine the size, surface properties, functionality, stability, and morphology. Followed by testing the release kinetics for the material after final loading with VD<sub>3</sub> (MSNM-Mg-VD<sub>3</sub>) in a phosphate buffer solution at pH 7.4, simulating bloodstream. Finally, the MSNM-Mg was investigated as a nano-detoxicant for the adsorption of Pb and 2,4DCPh from humans. The adsorptive behavior of VD<sub>3</sub> and the toxic compounds (Pb and 2,4DCPh) on the surface of the MSNM were studied using various isothermal models. Regeneration experiments for the spent materials were inspected with pH variation. Our findings showed that a stable SNM was formulated with a Z-potential of -36 mV compared to -30 mV before

modification, with 7 nm an average size. The material becomes less porous with a BET surface area reduction from 40 m<sup>2</sup>/g to 28 m<sup>2</sup>/g after modification to confirm successful anchorage of magnesium citrate on the surface. Although, the MSNM-Mg- VD<sub>3</sub> had the highest stability with -41 mV zeta-potential. A complete release of VD<sub>3</sub> was revealed after 5 hours, showing lower diffusivity ( $D_{eff}$ ) and better-controlled release compared to direct physical administration of VD<sub>3</sub>. Additionally, the adsorption isotherms for MSNM revealed a multi-layer adsorption behavior (BET) compared to a monolayer adsorption for the material before the primary activation step, which maximizes the effect of the modification on enhancing VD<sub>3</sub> adsorption. The MSNM-Mg showed an outstanding result in adsorption of Pb & 2,4DCPh individually with 388 mg/g and 5600 mg/g adsorption capacity, compared to 121 mg/g and 300 mg/g maximum adsorption capacity for the SNM, showing a multi-layer adsorption behavior represented by Freundlich and BET models respectively. The adsorption kinetics for both Pb and 2,4DCPh required only 10 min to attain equilibrium. The study showed an excellent recovery rate of over 90 % for the two adsorbents after three regeneration cycles. These findings support our assumptions that MNM could be an excellent adsorbent for Pb and 2,4DCPh, with a great recovery percent. These novel results reflect the importance of the unique surface modification technique in enhancing the stability of the modified nanomaterial and activate the surface energy toward maximizing the adsorption affinity of the nanomaterial towards the adsorbents.

# CHAPTER 1

## INTRODUCTION

### 1.1 Background

Starch, a naturally abundant polysaccharide derived from sources such as cereals (e.g., rice, wheat, corn, barley), tubers (e.g., potatoes, cassava), and legumes (e.g., peas, beans). It is considered a cornerstone of both food science and industrial applications due to its biocompatibility, biodegradability, and functional versatility (Ai et al., 2024; Y. Sun et al., 2025). Structurally, starch is composed of amylose (linear) and amylopectin (branched), with the ratio varying depending on the botanical source, influencing its physicochemical properties and suitability for various applications. High-amylose starches, for instance, offer enhanced gel strength and viscosity, making them valuable in specialty foods and industrial processes (Chavan et al., 2021, Montoya-Yepes et al., 2023).

In the food industry, starch is widely used for its thickening, stabilizing, and gelling abilities, contributing to desirable product attributes such as mouthfeel and stability (Chavan et al., 2021). Its renewable and biodegradable nature further positions it as a sustainable alternative to synthetic materials (Schmiele et al., 2019). Recently, advances in nanotechnology have enabled the transformation of starch into starch nanoparticles (SNPs), unlocking unique properties such as increased surface area, improved mechanical strength, and enhanced interaction capabilities with other molecules (Torres & De-la-Torre, 2022). These nanoparticles, typically ranging from 10 to 100 nm, can be synthesized via “top-down” (e.g., milling, ultrasonication) or “bottom-up” (e.g., precipitation) approaches, each affecting the resulting particle’s properties (Apostolidis et al., 2023).

Starch nanoparticles have garnered significant attention for their potential as carriers for micronutrients (notably vitamin D<sub>3</sub> and magnesium), controlled release systems, and food preservation agents (Alves et al., 2021; Hasanvand et al., 2015, 2018a). Their biocompatibility, ability to form hydrogen bonds and electrostatic interactions, and capacity for surface modification make them ideal for encapsulating and delivering sensitive bioactive in food matrices. However, native starch nanoparticles face challenges: poor stability under certain conditions, low solubility in non-aqueous media, and a tendency to aggregate or degrade (Rodrigues Arruda et al., 2025).

To address these limitations, surface modification through chemical (e.g., grafting, oxidation) or physical means (e.g., ultrasonication) has become a critical strategy (Marta et al., 2023). Modification of starch nanomaterials with agents like magnesium citrate can enhance their stability, dispersibility, and affinity for both micronutrients and toxicants. Such modifications not only improve nutrient delivery and controlled release but also expand their utility as sorbents for hazardous substances like lead and 2,4-dichlorophenol, addressing food safety and environmental concerns (Chacon et al., 2024).

The global prevalence of vitamin D<sub>3</sub> and magnesium deficiencies, which contribute to skeletal, cardiovascular, and metabolic disorders, underscores the need for effective delivery systems. Encapsulating these nutrients in modified starch nanoparticles can enhance their bioavailability, regulate release, and protect them from degradation, offering a promising solution for food encapsulation and public health.

Lead and 2,4-dichlorophenol (2,4-DCPh) are pervasive environmental pollutants that pose serious health risks worldwide. Lead contamination commonly

occurs through polluted soil, water, and food sources, leading to neurotoxicity and developmental disorders, especially in vulnerable populations. Meanwhile, 2,4-DCPh, a toxic degradation product of herbicides, accumulates in fruits, vegetables, and animal tissues, exhibiting carcinogenic and immunosuppressive effects. Traditional methods (like; chemical precipitation, adsorption via activated carbon, chemical oxidation) for removing these contaminants are often costly, inefficient, or environmentally unsustainable. Therefore, developing safe, eco-friendly, and cost-effective adsorbent materials is essential for reducing human exposure and safeguarding public health (Cechinel et al., 2014; Ghaffari et al., 2014; B. Liu et al., 2020; Neelgund et al., 2022).

## **1.2 Rationale of the Study**

Despite advances in starch nanoparticle technology, significant gaps remain in optimizing their functionality for dual roles: efficient delivery of bioactive nutrients and effective adsorption of toxic compounds. Most existing methods for producing and modifying starch nanoparticles are either complex, yield non-uniform particles, or fail to achieve the desired stability and performance in real food systems. Moreover, the synergistic impact of co-encapsulating both vitamin D<sub>3</sub> and magnesium within a single, surface-modified starch nanocarrier has not been fully explored.

Human exposure to toxic compounds such as lead and 2,4-dichlorophenol (2,4-DCPh) remains a significant public health concern, particularly through the ingestion of contaminated food and water. Lead contamination can result from various sources, including polluted soil, water, and the use of lead-glazed or soldered containers, and is especially harmful to the brain and nervous system, posing heightened risks for vulnerable groups such as children and pregnant women. Similarly, 2,4-DCPh, a degradation product of widely used herbicides and industrial chemicals, is frequently

detected in the environment and has been found in the urine of over 80% of the U.S. population, indicating widespread exposure (Cai et al., 2023; Xiaoyun Ye, Lee-Yang Wong, Xiaoliu Zhou & Division, 2014). Chronic intake of 2,4-DCPh is associated with liver and kidney toxicity, immunosuppression, and potential carcinogenicity, and acute exposures have resulted in fatalities through both ingestion and dermal absorption. Given the persistence and bioaccumulation of these pollutants in food crops, animal tissues, and water supplies, there is an urgent need for safe, eco-friendly, and cost-effective detoxification strategies. Starch-based nanomaterials offer a promising solution due to their biocompatibility, biodegradability, and low production cost. Despite this potential, up-to date there has been no reported attempts to use starch nano-adsorbents for 2,4-DCPh removal, and only limited studies have explored starch-based materials for lead detoxification.

This study combined native and high-amylose corn starches in one-to-one ratio, processed via ultrasonication and subsequently modified with magnesium citrate, to generate a starch-based nanomaterial with enhanced adsorption capacity toward vitamin D<sub>3</sub>, and magnesium, and demonstrating a controlled release property. The dual functionality of these modified nanoparticles which are as nutrient carriers and as sorbents for toxicants, addresses both nutritional and food safety challenges, offering a sustainable, scalable, and eco-friendly solution for the food industry.

### **1.2.1 Problem Statement**

Previously used Starch Nano Materials (SNM) have low stability in terms of size and zeta potential, they lack proper characterization using AFM, BET surface area analyzer, XRD, SEM, and Zeta-potential. Besides, without proof for efficient application (Hasanvand et al., 2015, 2018a). Limited research has investigated the

release performance for  $VD_3$  and failed to determine the diffusion coefficient ( $D_{eff}$ ) using Fick's law. Based on our knowledge there is limited research that study the use of SNM as detoxicant for 2,4DCPh removal. Besides, the literature that discussed SNM as a chelator either for Pb or 2,4DCPh removal from humans is still scarce.

Starch nanoparticles, while promising as food-grade carriers and adsorbents, are limited by poor stability, low solubility in non-aqueous environments, and insufficient affinity for both micronutrients and toxicants. There is a critical need for a robust, scalable, and safe modification strategy that enhances the functional properties of starch nanoparticles, enabling efficient encapsulation and controlled release of bioactive like vitamin  $D_3$  and magnesium, while also providing effective and safe adsorption of hazardous contaminants (Pb and 2,4DCPh) from humans.

### **1.2.2 Aim & Objectives**

This research is aimed at formulating and characterizing a stable starch nanomaterial that is prepared ultrasonically from native corn starch and high amylose corn starch (1:1 ratio) and further modified with magnesium citrate as a primary functionalization step. The resulting modified nanocarrier was later investigated for multiple applications (as a nanocarrier for  $VD_3$  in addition to magnesium, and as nano detoxicant for Pb and 2,4DCPh).

Objectives:

1. To produce a stable corn starch nano material (SNM) using ultrasonication followed by surface modification of the SNM using magnesium citrate with 1:12 magnesium oxide to citric acid ratio to produce modified starch nanomaterial with magnesium (MSNM-Mg).

2. To characterize the physical properties and functionalities of the (MSNM-Mg) as a nanocarrier for both vitamin D<sub>3</sub> and Mg simultaneously by analyzing the physical properties and functional performance of magnesium-functionalized mixed starch nanomaterials (MSNM-Mg) as nanocarriers for the simultaneous delivery of vitamin D<sub>3</sub> and magnesium using AFM, zeta potential, BET, XRD, and FTIR analyses.
3. To analyze the controlled release of VD<sub>3</sub> from the MSNM-Mg-VD<sub>3</sub>, using Fick's diffusion model to calculate the diffusion coefficient,  $D_{eff}$ .
4. To evaluate the MSNM-Mg as a nano adsorbent for the detoxification of Pb and 2, through batch adsorption studies and modeling using Langmuir, Freundlich, and BET isotherms.

### 1.2.3 Hypothesis

This research hypothesis is that the ultrasonically prepared starch nanomaterial, formulated using 1:1 ratio of native corn starch and high amylose corn starch and modified with magnesium citrate, will exhibit enhanced stability, size, and demonstrate efficacy in various applications, including:

1. Serving as an effective nanocarrier for both VD<sub>3</sub> and magnesium (Mg), maintaining their solubility and bioavailability, with proofing high adsorption capacity and controlled release.
2. Functioning as a potent nano-adsorbent for the detoxification of highly toxic compounds, such as lead (Pb) and 2,4-dichlorophenol (2,4DCPh), demonstrating maximum adsorption capacity and fast kinetics (10 min), maintaining around 90% regeneration of the material up to three cycles.

### 1.3 Thesis Organization (Framework)

The thesis is composed of four chapters in addition to general introduction and general conclusion.

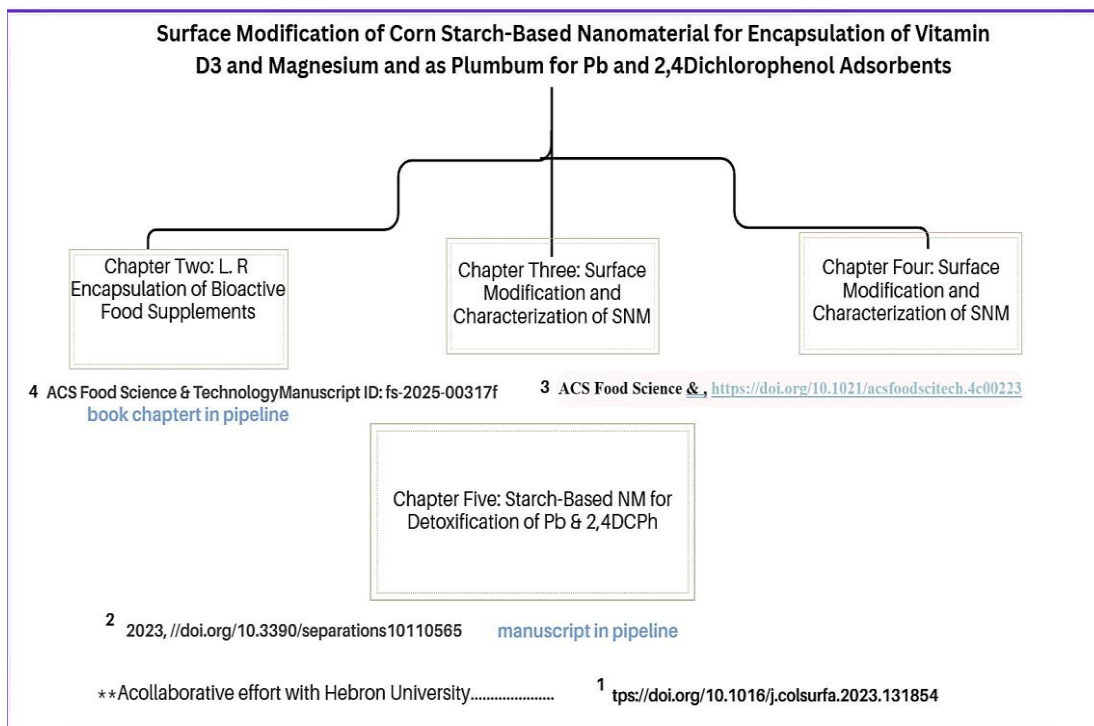


Figure 1.1 Thesis organization

## CHAPTER 2

### LITERATURE REVIEW

#### 2.1 Introduction

Vitamin D<sub>3</sub> (cholecalciferol) is a critical fat-soluble nutrient essential for human health, particularly for its role in calcium homeostasis, bone mineralization, and immune regulation. It enhances intestinal absorption of calcium and phosphorus, supports neuromuscular function, and reduces inflammation linked to chronic diseases such as cardiovascular disorders and depression. Despite its importance, Vitamin D<sub>3</sub> faces significant bioavailability challenges due to its extremely low water solubility (mole fraction solubility of  $1.03 \times 10^{-6}$  in water), which limits its dispersion and absorption in aqueous physiological environments. This insolubility, combined with rapid degradation in the gastrointestinal tract, often results in inadequate systemic delivery, necessitating innovative delivery systems to improve its stability and efficacy (Silva et al., 2024; Zhu et al., 2024).

VD<sub>3</sub> is characterized by high sensitivity to heat, light, and environmental conditions, Magnesium on the other hand have poor chemical stability (Bajpai et al., 2018; FAO (Food and Agriculture Organization) & WHO (World Health Organization), 2001). They can be thermally and chemically degraded throughout their manufacturing cycle, from harvesting to final storage, not to mention handling and transportation. Additionally, their biological functions are affected by physiological conditions inside the body while traveling in the gastrointestinal tract (Afzal et al., 2024; Joye et al., 2014).

With the growing demand for healthy foods, more emphasis on new processing technologies appeared, to develop novel and functional products with improved health benefits (Afzal et al., 2024). Currently, nanotechnology has entered this domain and improves the physicochemical stability and biological efficacy of bioactive compounds (Nsairat et al., 2023; Pateiro et al., 2021; Teng et al., 2023). Nano-objects are defined as having at least one dimension varying from 1–100 nm and therefore influencing a size-dependent property (Khan et al., 2019). The surface area to volume ratio and surface energy of a material increase as its dimension decreases from bulk to nanoscale (Butz, 2017; Khan et al., 2019).

The ratio of the active biological material encapsulated inside the nano-capsule to the total components of the core defines the encapsulation efficiency (EE) (Brunetti & Felice, 2016), while encapsulation loading (EL) is another term used to express the mass ratio of core to total nanoparticle. Both terms affect nano-capsule stability and release performance (Hasanvand et al., 2015, 2018b; Pardeshi et al., 2020; Talón et al., 2019; Yun et al., 2021).

Both the physical and chemical qualities of the polymer and the microcapsules have an impact on the release of bioactive substances from the capsule to the intended organ. Either a modified form (controlled release) or an immediate form (burst release) of this may occur (Mehtani et al., 2019). Therefore, increasing the stability of nano-capsules is necessary to ensure their sustained release. Stability is maintained by increasing the resistance of nanocarriers; accordingly, this lowers the diffusivity of bioactive compounds in the body fluid. The Fickian diffusion model was used to validate both release behavior and kinetics (Boostani et al., 2021; Nile et al., 2020).

Carbohydrates, fats, and proteins are organic materials commonly used to prepare encapsulant materials (Mandal & Ray Banerjee, 2020). One substance or a mixture of several compounds was used for the nano-capsule modification. The choice was made according to the bioactive material and food applications. The core material is combined with an encapsulant (wall) to form what is called encapsulation following different methods (Mandal & Ray Banerjee, 2020), either chemical, physical, or a combination of both techniques are used to perform nanoparticles. Emulsification, coacervation, inclusion complexation, and emulsification-solvent evaporation are all processes that fall under this category (Yun et al., 2021).

Despite the multiplicity and diversity of these methods, it is not possible to use a single method for all bioactive compounds and different food applications (Baldwin et al., 2011). Multiple factors were discussed before determining the best method of application. The key influence of the chosen wall material (encapsulant), in addition to safety, is the cost (Meer et al., 2015; Oh et al., 2020), as well as the site of release (targeted organ), and the compatibility between bioactive material and wall material (Khan et al., 2019; Pateiro et al., 2021).

Carbohydrates are the most widely utilized encapsulating materials in food and pharmaceuticals (Nile et al., 2020; Outline, 2015). Pectin, chitosan, glucans, and cellulose are starch derivatives. It is natural, biodegradable, safe, biocompatible, and sustainable, with special mechanical properties. The active hydroxyl groups in starch interact with hydrophilic and hydrophobic compounds, resulting in a high-heat-stability solution (Hethnawi, 2023). As a nanocarrier, it forms a suitable shell for entrapping sensitive bioactive compounds (Chen et al., 2019; Hasanvand et al., 2015, 2018; Kemper et al., 2005; Oh et al., 2020), and thus promote slow release and inhibits burst release. Surface modification of the shell wall was proposed to ensure

nanoparticle stability and sustained release (Chen et al., 2018). This can be achieved by blending starch, cross-linking, or surfactants (Sadeghi et al., 2017).

## **2.2 Starch**

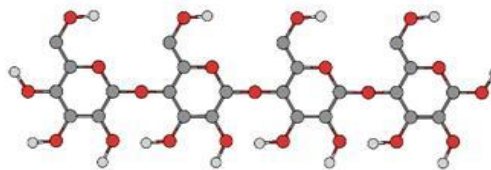
### **2.2.1 Starch Identification and Composition**

Plants store energy in starch, a natural, renewable, and biodegradable polymer (Iskalieva et al., 2024; Schmiele, 2019; Zhu et al., 2024b). After water, it ranks as the most common type of biomass (BeMiller & Roy, 2009).

Glucose is the building unit of starch. It is hydrolyzed by amylase, which transforms the stored starch granules into glucose (Schmiele, 2019; Parker & Ring, 2001). Starch can be easily separated in granular form by gravity sedimentation, centrifugation, and filtering, and then exposed to different changes; chemical, physical, or enzymatic with further processing steps. As a result, it is one of the most cost-effective commodity goods (Mittu et al., 2024). Starch is one of the most important biopolymers owing to its abundance and low cost. In 2010, surveys revealed that the demand for starch increased by 17 % compared to that of other polymers. By 2020, global demand will rise by 1.3 million tons (MT) (Hanisah Kamilah et al., 2020).

Plant cells generate two forms of starch: amylopectin and amylose as in Figure 2.1. Amylopectin, which makes up 70-85% of common starch, is made up of glucose units connected in linear chains by  $\alpha$ -1,4 glycosidic bonds and is tightly branched at the  $\alpha$ -1,6 locations by short chains of glucose spaced 10 nm apart along the molecule's axis. (Temitope Fatokun, 2020) . Table 2.1 presented comparison between amylose and amylopectin in terms of Molecular weight, solubility, dilute solution, complex formation, gel, degree of polymerization and so on.

(a) Amylose



(b) Amylopectin

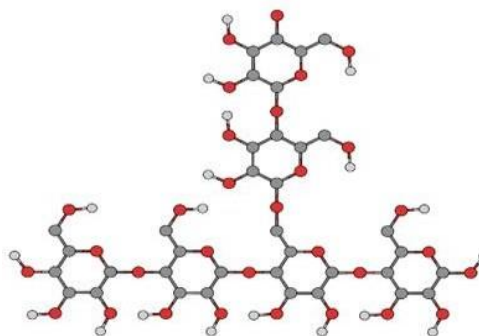


Figure 2.1. (a) Structural units of starch amylose, and (b). Amylopectin: red is oxygen atom, white is hydrogen atoms, and grey is carbon.

Table 2.1 Comparison between amylose and amylopectin in starch

Item	Amylose	Amylopectin	Ref
1. Mw- $\text{gmol}^{-1}$	$10^5$ - $10^6$	$10^7$ - $10^9$	(Alcázar-Alay & Meireles, 2015; Forssell et al., 2002; Liu & Han, 2005; M.Schmiele, 2019)
2. Dilute solutions	Unstable	Stable	
3. Solubility	Variable	Soluble	
4. Complex formation	Favourable	Unfavourable	
5. Gel	Stiff, irreversible	Reversible	
6. Films	dendrite feature	Cluster network with an amorphous background.	
7. Degree of polymerization	1500-6000	$3 \times 10^5$ to $3 \times 10^6$ Stable	
8. Diffraction	Amorphous	Crystalline	
9. Degree of crystallinity %	~30%	~15%	
10. Films crystallinity after heat treatment	crystalline	Entirely amorphous.	
11. Digestibility (b-amylase)	100%	60%	

The starch molecular weight is affected by the ratio between amylose to amylopectin, and it is detected by the plant origin of the starch (Parker & Ring, 2001). The average molecular weight for amylose is  $10^5$ - $10^6$   $\text{g mol}^{-1}$ , while amylopectin is  $10^7$ - $10^9$   $\text{g mol}^{-1}$  (Brouillet-Fourmann et al., 2003; Schmiele, 2019). As aforesaid, the starch characteristics are determined by the starch origin to a certain extent (Morán et al., 2021; Temitope Fatokun, 2020; Tester et al., 2004). It is noticed that this variation may rise according to different climatic or geographical conditions, and not specified within the same family of genus (Montoya-Yepes et al., 2023).

### **2.2.1(a) Native and High Amylose Corn Starch**

Native cornstarch consists of a very fine, white powder mainly composed of two polysaccharides: amylose and amylopectin (Ai & Jane, 2024; Sadeghi et al., 2017). The ratio of these two constituents is different in the different types of corn, although they generally contain 25% amylose and 75% amylopectin (Ai & Jane, 2024; Sadeghi et al., 2017). This is one of the most common starches used for thickening, stabilizing, and moisture retention in sauces, soups, and baked products, especially gluten-free ones. It is prepared through cleaning, milling, and drying of the endosperm of maize to result in a non-GMO product that has a neutral taste and odor (Siró et al., 2008). The gelatinization of native corn starch lies between 80 to 85 °C, retaining its properties well in various applications such as animal feeds and pharmaceuticals (Ratnayake & Jackson, 2008).

High amylose corn starch is obtained from those maize strains which contain a higher level of amylose, probably ranging from 50% to 90% of the total starch (Obadi et al., 2023). This starch is characterized by the ability to form hard gels and to be less digestible compared to normal starch

It is well established that amylose content controls the thermal stability of maize starch due to modification of gelatinization temperature, thermal characteristics, resistance to retrogradation, and structural interactions within the starch granules (Ai & Jane, 2024; Obadi et al., 2023). This knowledge is important for maximum utilization of starch in dietary and other industrial applications. The higher amylose content and more ordered V-type crystalline structures in corn starch contribute to its high thermal stability, characterized by higher gelatinization temperatures, wider gelatinization ranges, and resistance to breakdown. Such properties are highly welcome in food and related industrial applications involving heat stability (Huang et al., 2022; Nakamura, 2015).

The high amylose starches could also develop improved thermal stability because of the V-type crystalline structure that they form. Besides, these kinds of starches are resistant to digestion; therefore, resulting in resistant starch nanoparticles with high potential for usage in pharmaceuticals and functional foods, where controlled release is necessary (Obadi et al., 2023). Higher amylose levels consequently result in smaller, more crystalline, less digestible nanoparticles, which are ideal for specific applications (Obadi et al., 2023; Seung, 2020).

The high-amylose starches also exhibited enhanced heat stability because of the formation of V-type crystalline form. Such starch nanoparticles obtained are also poorly digestible, thus giving resistant starch nanoparticles suitable for control release for drug and functional food purposes. Overall, with increased amylose content, the resultant nanoparticles had smaller size, more crystalline, less digestible characteristics, hence more useful in certain applications (Obadi et al., 2023; Seung, 2020).

### **2.2.2 Physicochemical Properties: Viscosity, Thermal Stability, Crystallization, Retrogradation**

Viscosity, heat stability, crystallinity, and retrogradation are the physical features that distinguish each type of starch, resulting in a wide range of starch usage in foods based on their attributes and behavior. These properties are generally influenced by the size of the starch grains, the type of crystallinity, as well as the amylose-to-amylopectin ratio (Rodrigues Arruda et al., 2025).

Gelatinization is defined as breaking the molecular order of granules and melting the crystallites when heating starches in excess water (>1:2 starch: water) over a particular temperature, known as the gelatinization temperature. When less water is available (<1:2 starch: water), gelatinization is postponed to higher temperatures (Waterschoot et al., 2015). Thermal treatments performed on starch aqueous solutions may lead to the formation of novel structures and characteristics (Lacerda et al., 2024).

Two kinds of starch are available in the market: native and modified starch. Table 2.2 represented the main differences between native and modified starch. Native starches maintain the properties that they already have in the plants from which they are harvested (Kemper et al., 2005). Modifications, including physical, chemical, enzymatic, or their combinations enhance the properties of native starches to satisfy technical needs (Marta et al., 2023).

Table 2.2 Comparison between native and modified starch

Type of starch	Morphology	Amylose content w/w%	Degree of crystallinity	Ref
Native high amylose corn starch	Polygonal and Angular	42.6 – 70	19.2 ±1.4	(Alcázar-Alay & Meireles, 2015)
High Amylose corn starch	Angular	70%	19±1.4	(Qin et al., 2016)
Potato starch	Smooth-surfaced, oval, and irregular	20.1 – 29.5	45.9±0.6	(Alcázar-Alay & Meireles, 2015; Qin et al., 2016)

Modified starch typically contains more amylose, increased thermal stability, and modified crystallinity, chemical composition, and geometry, all of which lead to increased utilization in industry and novel applications (Govindaraju et al., 2021; Tharanathan, 2005). The investigation of physicochemical and thermal characteristics of native and modified starch serves several functions. **Table 2.3 represented the differences between native and modified starch in morphology.** Tharanatha (2005), focused on continuous functionalization of starch to yield new products. These innovations are being increasingly employed across a diverse array of industrial applications, resulting in substantial value addition (Tharanathan, 2005).

Table 2.3 Scanning electron microscopy, for different types of starch

Scanning electron microscopy of starch granules			
Type of the starch		Morphology	Ref
Maize	Native	Angular with round edges	(Dai et al., 2018; Wei et al., 2018)
	Modify by ball-milled acid hydrolysis	- Were several holes in the surface of the raw starch granules. - The granule structures of ball milling-45 starch were partially damaged, and the starch contents leaked out of the granules.	
Potato	Native	- Oval, smooth Potato. - Smooth-surfaced, oval, and irregular	(Alcázar-Alay & Meireles, 2015; Vafina et al., 2018; Wang et al., 2019)
	Modify by enzyme	Cracks and slits are comparatively more susceptible to hydrolysis than the unheated sample.	
Corn	Native	- Polygonal, Rough outer surface with few pores unevenly distributed. - Polygonal and Angular.	(Alcázar-Alay & Meireles, 2015; Evers & McDermott, 1970; Wang et al., 2019)
	Modify by enzyme	- Pores, unevenly distributed, slit and cracks. - Cracks and pores could be seen on Surface.	

### 2.2.3 Morphological Characteristics

The microscopic size of starch granules ranges from 0.1- 200µm, and their morphology varies based on the botanical source, such as oval, ellipsoidal, spherical, smooth, angular, or lenticular (Alcázar-Alayan & Meireles, 2015; Lacerda et al., 2024). Size distribution can be either unimodal or polymodal. These granules can be found either alone or in groups of amyloplasts (Schmiele, 2019). Before microscopic examination, starch granules are normally isolated either by washing, purification, or centrifugation (Alcázar-Alay & Meireles, 2015; Niu et al., 2019). A central line called the hilum, or "Maltese cross" is common in granule morphology. Each starch granule may include one or more Maltese crosses, which lowers the starch granule's

birefringence potential (Alcázar-Alay & Meireles, 2015; Chen et al., 2018; Olsson, 2013; Pérez & Bertoft, 2010).

The molecular shape of starch refers to how amylose and amylopectin are organized within starch granules in either raw (native) or modified starch. However, this shape has a substantial influence on the functional qualities of starch, as well as the physicochemical features and characteristics (Schmiele, 2019). In addition, it is suggested to consider the distribution of amylopectin chain length as a limiting factor in understanding the physicochemical and functional characteristics of starch (Schmiele, 2019; Zhang et al., 2006).

The structure of starch granules is extremely complicated. Variations in the composition (alpha-glucan, moisture, lipid, protein, and phosphorylated residues) and structure of the components contribute to the complexity (Rasmi et al., 2024; Tester et al., 2004). In addition, there is an additional level of variation that indicates how amorphous and crystalline elements are connected. Although significant knowledge obtained over the previous century has led to fresh perspectives on this key element of many food and non-food products, there is still much to learn about the complications of starch granules (Tester et al., 2004).

Starch has a "double helix" shape which comprises two types of molecules: linear and helical amylose and branched amylopectin ( Nakamura, 2015). V amylose is the natural and spontaneous ability of amylose to form single helical molecular inclusion complexes ( Tufvesson et al., 2003). It also features a core hydrophobic cavity that is linked by amorphous sections of the polysaccharide chains, making the complexes very resistant against acidic hydrolysis and potentially useful as a platform

for the encapsulation of hydrophobic compounds (Biais et al., 2006; Heinemann et al., 2003).

Although it is difficult to provide a complete description of starch morphology in terms of size, shape, amount, and orientation of ordered chain assemblies, as well as the precise nature of the amorphous domains, there is a growing recognition of the relationship between the internal structure (molecular and super molecular) and macroscopic properties of starch. Information acquired from sensitive polymer structure probes offers evidence for varied levels of chain organization, not only within the granule but also in both pharmaceutical and food applications(Ai & Jane, 2024).

#### **2.2.4 Potential Use**

Native starch is not commonly used or utilized in industry (Garcia et al., 2024). Most original starches have limited direct applicability since they are unstable in terms of temperature, pH, and shear stress (Serge Perez, 2009). Native starches are susceptible to destruction and retrogradation(Haq et al., 2019) Moreover, many starch particles are inert, and resistant to water and enzyme breakdown therefore they lack functional properties. Native starches are commonly changed to generate specific properties, including solubility, smoothness, and adhesion, with resistance against high temperatures at industrial operations (Alcázar-Alay & Meireles, 2015; Singh et al., 2007; Sweedman et al., 2013).

Many changes have been implemented to modify starch characteristics and gain certain functions. Many different methods can be employed to alter starch, including physical processing, chemical reactions (such as cross-linking, acetylation, carboxymethylation, hydroxy ethylation, oxidation, and partial hydrolysis), or enzymatic degradation. Depending on the modification technique, the properties of the

final result will be significantly associated with the initial amylose/amylopectin ratio and indirectly influenced by the starch's origin (Alcázar-Alay & Meireles, 2015; López et al., 2010). Modified starch hydrophilic polymers are suitable for controlled drug delivery systems because they are low-cost, accessible, biocompatible, and have good *in vivo* performance (Outline, 2015).

In solution, starch tends to precipitate; therefore, it should undergo some modifications before being used in food processing. Moreover, minor alterations can convert this material into outstanding manufacturing results (Schmiele, 2019).

#### **2.2.4(a) Encapsulation**

Encapsulation is a process of packing active ingredients in tiny capsule-like particles that release their contents in specific proportions and targeted places over long periods (Schmiele, 2019; Nanda et al., 2024; Zhu et al., 2024). Flavours, beverage clouds, creamers, and vitamins are all encapsulated in starch derivatives (Bertoft, 2017; Kemper et al., 2005; Schmiele, 2019; Madene et al., 2006). As an example, a common procedure involves dispersing the oil in a solution with approximately four times the amount of encapsulant, then homogenizing the mixture and spray drying it. Extrusion, fluidized bed addition, and drum drying are three additional mechanical encapsulation methods. Coatings are formed, the emulsion is stabilized, and a dry matrix that inhibits oil is finally generated by the starch analogs. The encapsulant reduces volatile loss during drying, as well as oil oxidation during storage (Brandelli et al., 2019; Jafari et al., 2008).

Encapsulation of genistein (a kind of isoflavone) by amylose inclusion complexes, for example, enhanced *in vivo* bioavailability in a rat model, as mentioned by other scholars (Cohen et al., 2011; Zhu, 2017). Multiple researchers have

investigated the encapsulation of polyphenols, vitamins, oils, carotenoids, enzymes, tastes, live cells (e.g., probiotics), and other substances for targeted delivery (Chin, Mohd Yazid, et al., 2014; Zheng Li et al., 2009; Mun et al., 2015; Zhu, 2017).

Increasing interest in using bioactive compounds as functional ingredients in innovative food formulations presents a challenging area for the application of microencapsulation technologies. Many existing procedures are limited by their high production costs and a lack of food-grade ingredients (Jampilek et al., 2019).

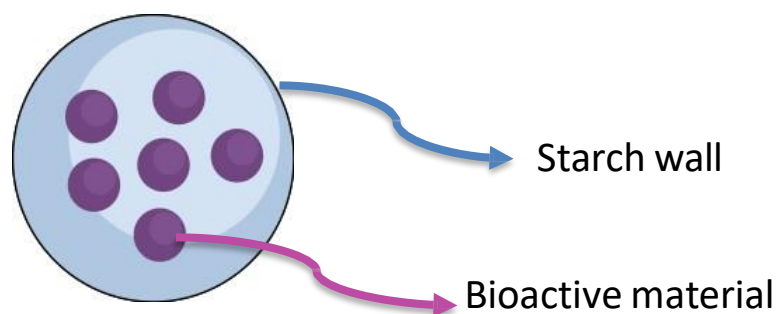


Figure 2.2 Resistant starch-encapsulated probiotics

Encapsulation is a process that protects the bioactive material inside a polymer (such as proteins, lipids, polysaccharides, or a combination of two or more). These alternatives are used to fabricate the capsule wall material (As et al., 2004; Jafari et al., 2008; Katouzian & Jafari, 2016; Chengzhen Liu et al., 2017; Maurya & Aggarwal, 2019; Zhu, 2017). Starch is a polysaccharide that undergoes some modifications and can encapsulate hydrophobic and hydrophilic ingredients as shown in Figure 2.3. It enhances the ability of hydrophobic materials to bind on it and makes the dispersion of bioactive material inside the starch easier (Acevedo-Guevara et al., 2018; As et al., 2004; Rostamabadi et al., 2019; Zhu, 2017). Bioactive materials such as flavours, vitamins, oils, and living cells (probiotics) could be hydrophobic or hydrophilic (Figure. 2.3). These materials are characterized by their low processing stability, low

water solubility, and low bioavailability. All factors were solved by encapsulation (Acevedo-Guevara et al., 2018; Lesmes et al., 2008; Maurya & Aggarwal, 2019; Rostamabadi et al., 2019; Zhu, 2017).

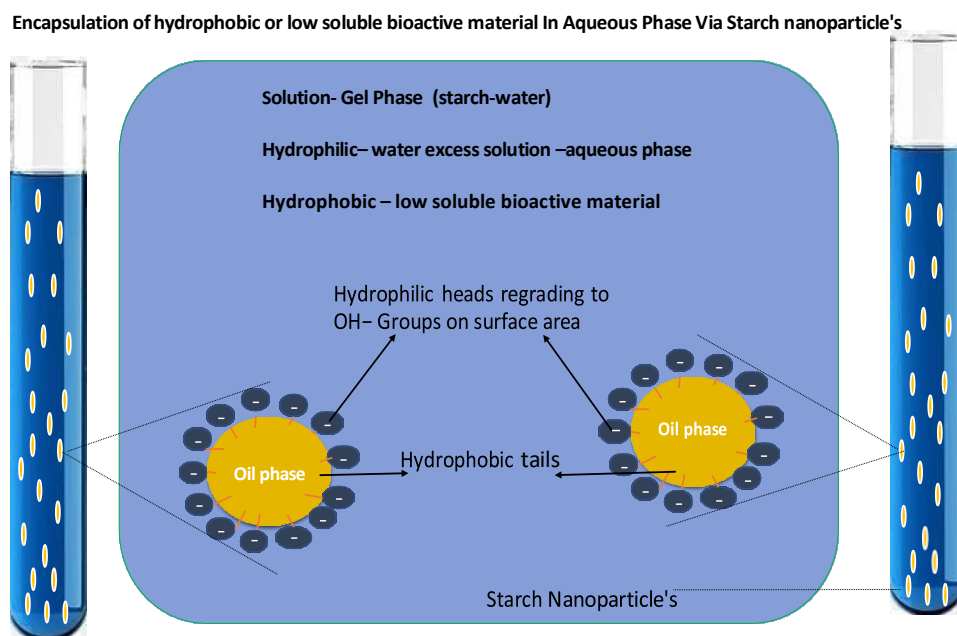


Figure 2.3 The figure shows encapsulation of hydrophobic or low bioactive material in an aqueous phase

Starch-based encapsulation material could be developed through different processes; spray drying, electrospinning, nano-emulsification, amylose inclusion complexation and ultrasonication (Zhu, 2017). According to the synthesis process, the starch nano system can be classified as either starch nanoparticles or starch nanocrystals (Kemper et al., 2005; Wei et al., 2018). Physical approaches, like ultra-high-pressure treatment, are used to control the nanoprecipitation of the gelatinized starch to gain starch nanoparticles (Farrag et al., 2018; Lecorre et al., 2012; Qin et al., 2016; Shi et al., 2011; Villa et al., 2019).

Furthermore, new and more efficient procedures are used to synthesize starch nanoparticles, including the precipitation of amorphous starch (Shi et al., 2011; Zhou

et al., 2014a; Shi et al., 2011; Zhou et al., 2014a), combining complex formation and enzymatic hydrolysis (Zhou et al., 2014b), that results in V-shape nanocrystals (i.e., complexed with lipid) and by micro fluidization. Those procedures are different yielding various properties, shapes, and crystallinity (Le Corre & Angellier-Coussy, 2014). (Table 2.4)

Compared with inorganic nanoparticles, SNPs are characterized by high rigidity, high specific surface area, multivariable morphology, high specific strength (Šturcová et al., 2005), and high amounts of hydroxyl groups on the surface of the nanoparticles. This leads to a favorable surface and favorable related chemical characteristics. In addition, they are prepared for derivatization and functional property integration. These advantages make SNP a suitable and unique solution for formulating nano capsules. These particles could be used in pharmaceuticals, foods, or any other industries with more attention (Molina-boisseau et al., 2005; Wei et al., 2018).

### **2.3 SNPs Structure and Synthesis protocol**

Nano-sized starch can be obtained using two different approaches; top-down and bottom-up (Mandal & Ray Banerjee, 2020) (Figure 2.5). Top-down technologies involve degradation procedures in which native starch granules are physically or chemically manipulated. On the other hand, bottom-up methods begin with the addition of a solvent to non-solvent starch molecules that dissolve and precipitate or employ other chemical treatments. Either one preparation protocol or a combination of two or more in a multi-treatment protocol, both techniques are valid (Mandal & Ray Banerjee, 2020; Wei et al., 2018).

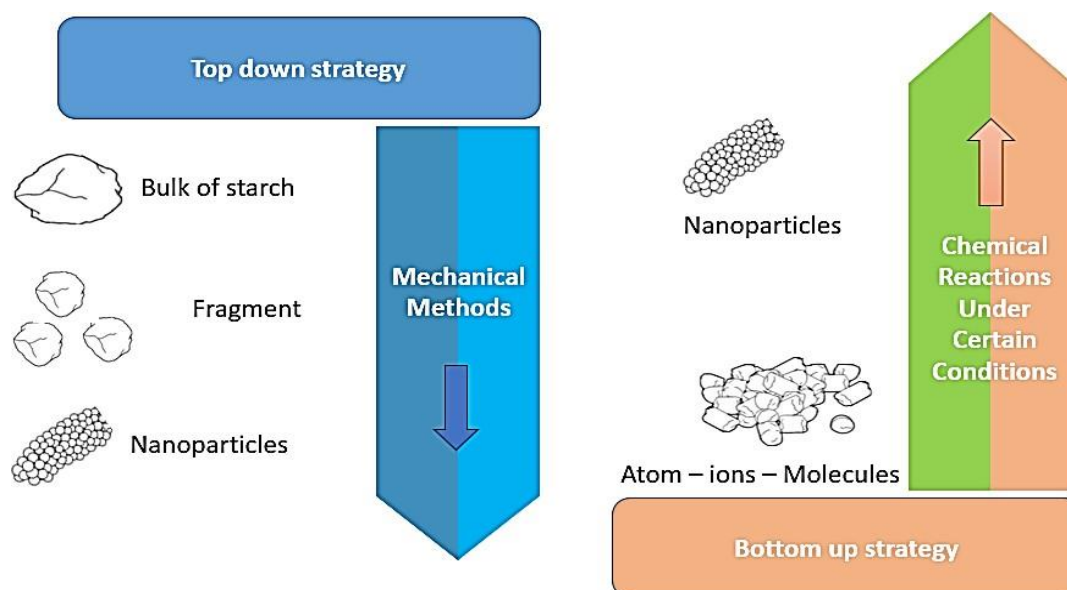


Figure 2.4 SNP's preparation approaches

Ma et al. (2008) created starch nanoparticles and used them to build a Nano capsule. They began with a solution of gelatinized starch in ethanol, and the yield was obtained by centrifugation and drying at 50 °C (Ma et al. (2008)). Recently, precipitation of DNA with starch in ethanol was performed by Ip et al. 2014, (Ip et al., 2014). Additionally, Hebeish et al. 2014, utilized polysorbate to modify starch nanoparticle production. Surfactants were used for the modification, yielding nanoparticles of smaller sizes (Hebeish et al. 2014). Table 2.4 defines the preparation methodologies of SNPs.

Table 2.4 SNP's preparation methodology; top-down and bottom-up

<b>Top-down</b> (Wei et al., 2018)	<b>Bottom-up (self-assembly)</b> (Wei et al., 2018)
Hydrolysis Acidic /enzymatic	Crystallization
<u>Physical Treatments</u> <u>such as ultrasound, extrusion, microfluidizer,</u> <u>milling, and gamma radiation</u>	Nanoprecipitation
	Emulsion Cross-Linking Emulsion